ChemComm

ROYAL SOCIETY OF CHEMISTRY

COMMUNICATION

View Article Online
View Journal

Check for updates

Cite this: DOI: 10.1039/d1cc02832d

Received 28th May 2021,
Accepted 15th June 2021

DOI: 10.1039/d1cc02832d

rsc.li/chemcomm

Facile proton-coupled electron transfer enabled by coordination-induced E–H bond weakening to boron†

Anthony Wong,[a] Arunavo Chakraborty,[a] Deependra Bawari,[b] Guang Wu,[a] Roman Dobrovetsky[b] and Gabriel Ménard*[a]

We report the facile activation of aryl E–H (ArEH; E = N, O, S; Ar = Ph or C_6F_5) or ammonia N–H bonds *via* coordination-induced bond weakening to a redox-active boron center in the complex, $[CoCp^*_2][(N(CH_2CH_2N(C_6F_5))_3)V(\mu\text{-}N)B(C_6F_5)_2]$ ($\mathbf{1}^-$). Substantial decreases in E–H bond dissociation free energies (BDFEs) are observed upon substrate coordination, enabling subsequent facile proton-coupled electron transfer (PCET). A drop of >50 kcal mol^{-1} in H_2N–H BDFE upon coordination was experimentally determined.

Key to several biological, catalytic, and energy-related transformations, PCET reactions describe any process involving proton transfer (PT) and electron transfer (ET) in stepwise or concerted (CPET) kinetic steps.[1] The most studied PCET mechanism, hydrogen atom transfer (HAT), is on the same "continuum" to – yet often distinguished from – related concerted processes (*e.g.* separated CPET) by the proximity of the H^+/e^- acceptor or donor sites;[2] however, the distinction between these mechanisms is often blurred.[1–4] In contrast to classic HAT examples (*e.g.* alkane C–H homolysis), separated CPET chemistry may be facilitated by the coordination-induced bond weakening (CIBW) of an E–H fragment (E = N, O, S, *etc.*) to a redox-active metal center, in turn lowering its bond dissociation free energy (BDFE) substantially (Fig. 1a).[5] The effect of CIBW may be seen at positions α[4–8] or downstream (β, γ, *etc.*)[9–13] of the metal center and may result in either spontaneous H_2 evolution or facile separated CPET reactions with H-atom abstracting (HAA) agents. Bullock,[4] Knowles,[10,11] and others[14,15] have utilized this effect to target catalytic PCET-enabled transformations, such as for NH_3 oxidation or conjugate amination reactions (Fig. 1a).

The effect of CIBW on modulating substrate E–H BDFE is governed by the metal's redox potential (E°), as well as the pK_a of the E–H fragment (which is influenced by the metal's Lewis acidity).[16] Thus, coordination of a protic E–H donor (*e.g.* H_2O, NH_3) to a classic redox-inactive Lewis acidic center (*e.g.* groups 1, 2, 13) may result in a substantial decrease in pK_a, but minimal change to overall BDFE due to a lack of available redox at the Lewis acid. We previously reported the synthesis and reactivity of a new borane tethered to a redox-active V^{IV} center, $[CoCp^*_2][(N(CH_2CH_2N(C_6F_5))_3)V(\mu\text{-}N)B(C_6F_5)_2]$ ($\mathbf{1}^-$, Fig. 1b).[17] While the V^V congener (**1**) displayed classic group 13 Lewis acidic behavior, compound $\mathbf{1}^-$ (V^{IV}) displayed reactivity indicative of "hidden" B^{II} radical character by virtue of the electron delocalization over the N bridge (Fig. 1b). In this report, we demonstrate how coordination of protic E–H donors to the main group B center results in substantial E–H CIBW and lowered BDFE due to the cooperative actions of the Lewis acidic (B) and redox-active (V^{IV}) centers. Facile PCET using HAA agents ($Y^\bullet$) and/or spontaneous $H^\bullet$ ejection are observed and presented here (Fig. 1b).

Our study began by exploring the E–H CIBW effects using an isostructural ArEH series (Table 1). We then expanded this to NH_3, a potential energy storage vector of interest to our lab.[12,18] We note that the BDFE values in Table 1 were selected in a common solvent, benzene, using reported experimental values or were calculated using DFT where needed. While benzene was chosen as the common reference solvent, for experimental reasons, not all reactions were performed in this solvent; therefore, this table is primarily used to highlight general trends. We initially probed the relative Lewis acidity of **1** (V^V) and $\mathbf{1}^-$ (V^{IV}) using the Guttman–Beckett method.[19,20] Using Et_3PO in bromobenzene, ^{31}P NMR chemical shift differences ($\Delta\delta_P$) revealed acceptor number (AN) values of 77.1 ($\Delta\delta_P$ = 29.1) and 13.9 ($\Delta\delta_P$ = 0.5) for **1** and $\mathbf{1}^-$, respectively (Fig. S35–S36, ESI†). These values are similar to $B(C_6F_5)_3$ for **1** and to $B(OMe)_3$ or $B(NMe_2)_3$ for $\mathbf{1}^-$ with the reduced acidity in $\mathbf{1}^-$ ascribed to the non-negligible spin density (13%) on B.[17,20,21] We note that

[a] Department of Chemistry and Biochemistry, University of California, Santa Barbara, CA 93106, USA. E-mail: menard@chem.ucsb.edu
[b] School of Chemistry, Raymond and Beverly Sackler Faculty of Exact Sciences, Tel Aviv University, Tel Aviv 69978, Israel

† Electronic supplementary information (ESI) available: Synthetic procedures, spectroscopic data, GC-TCD, XRD, CV, DFT. CCDC 2086944–2086950. For ESI and crystallographic data in CIF or other electronic format see DOI: 10.1039/d1cc02832d

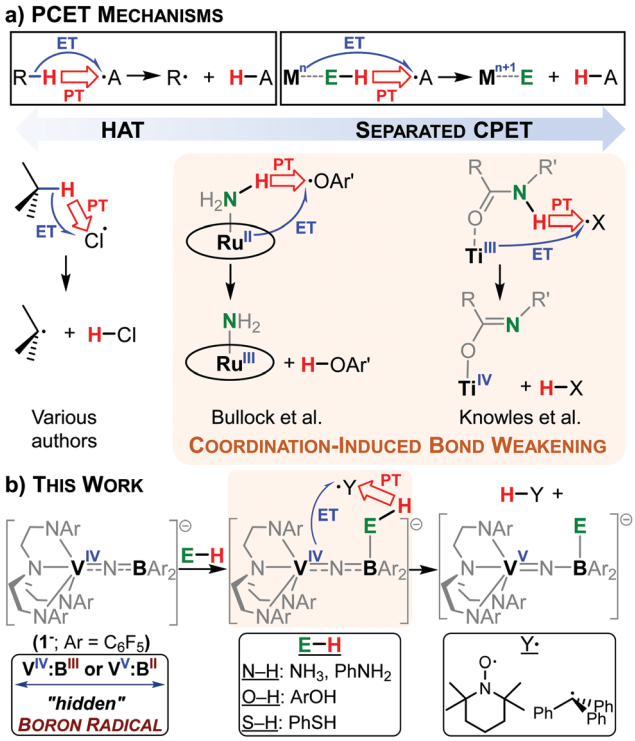

Fig. 1 (a) Common PCET mechanisms on a "continuum": hydrogen atom transfer (HAT, left box) and separated concerted proton–electron transfer (CPET, right box). Examples of each are shown with coordination-induced bond weakening (CIBW) effects highlighted for selected examples at α[4] and γ[10] positions to the metal center (see references for specific metal complexes used). (b) This work highlighting the facile E–H PCET reaction enabled by CIBW to a "hidden" B radical. The counter-cation in $\mathbf{1}^-$, $[CoCp^*_2]^+$, is omitted for simplicity.

Table 1 Reported[1,22] and calculated BDFE values for ArEH, NH_3, and HAA agents

Category	Compound	BDFE (kcal mol^{-1})	Medium	Comment
ArEH	C_6F_5**O–H**	78.9	Benzene	Calc.
	Ph**S–H**	81.6	Benzene	Exp. (ref. 1)
	PhH**N–H**	87.4	Benzene	Exp. (ref. 1)
NH_3	H_2**N–H**	99.4	Gas	Exp. (ref. 1)
HAA agent	TEMP**O–H**	65.2	Benzene	Exp. (ref. 22)
	Ph_3**C–H**	71.7	Benzene	Calc.

the paramagnetic nature of $\mathbf{1}^-$ may unpredictably affect this assigned AN value; therefore, this AN value is only tentative.

Treatment of **1** with C_6F_5OH or $PhNH_2$ in benzene revealed common ^{51}V and ^{19}F NMR resonances indicating the formation of the imine product, $(N(CH_2CH_2N(C_6F_5))_3)VNH$ (**2**), which was confirmed by independent synthesis. Other ^{11}B and ^{19}F NMR resonances suggest the formation of the products, $(C_6F_5)_2B$–EAr (Scheme 1 and Fig. S37–S42, ESI†).[23,24] This reactivity suggests coordination of the Lewis basic ArEH donor to the B center followed by rapid intramolecular deprotonation. No reaction was observed with PhSH.

We next probed the analogous reactions with the V^{IV} complex, $\mathbf{1}^-$. Treatment of $\mathbf{1}^-$ with an equivalent of C_6F_5OH

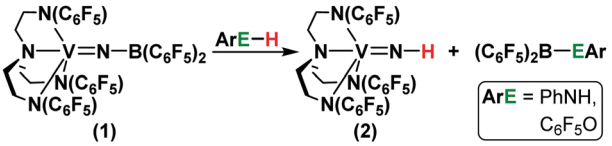

Scheme 1 Reaction of **1** with ArEH in bromobenzene.

or PhSH – having the lowest E–H BDFEs (Table 1) – in bromobenzene revealed the formation of major products with broad ^{51}V resonances in the NMR spectra centered at −272 (PhSH) and −302 (C_6F_5OH) ppm. A set of 6 (PhSH) or 9 (C_6F_5OH) major resonances were also observed in the ^{19}F NMR spectra, along with several minor byproducts, including the free tren ligand, as well as other unknown species (Fig. S46–S49, ESI†). Following workup, both major products (~50% yield each) were isolated and structurally characterized by single crystal X-ray diffraction (XRD) studies as the complexes **1-SPh** and **1-OC$_6$F$_5$** (Fig. 2a–c). Note that there were two molecules of **1-SPh** in the asymmetric unit; the average metrics were taken. Both complexes displayed significantly shortened V1=N1 bonds (1.661(avg) Å (**1-SPh**), 1.655(7) Å (**1-OC$_6$F$_5$**)) compared to $\mathbf{1}^-$ (1.776(4) Å) and are consistent with oxidation to V^V (1.703(4) Å (**1**)).[17] B(1)–S(1) (1.960(avg) Å) and B(1)–O(1) (1.476(10) Å) are similar to reported aryl-sulfide and -oxide bond lengths.[25,26] These reactions indicate formal loss of H• and attempts to detect possible H_2 formation by ^{1}H or ^{2}H NMR spectroscopy – the latter using the C_6F_5OD isotopologue – revealed no H_2 (or D_2) in either case (Fig. S47–S49, ESI†). GC-TCD experiments also did not reveal any H_2 formation (Fig. S66 and S67, ESI†).

The reaction of $\mathbf{1}^-$ with $PhNH_2$ was considerably more sluggish, perhaps due to its higher N–H BDFE (87.4 kcal mol^{-1}; Table 1). The ^{19}F NMR spectrum revealed a significant quantity of C_6F_5H produced suggesting a competing reaction pathway compared to the two previous reactions. The ^{51}V NMR spectrum featured some **2** and a broad resonance at −312 ppm,

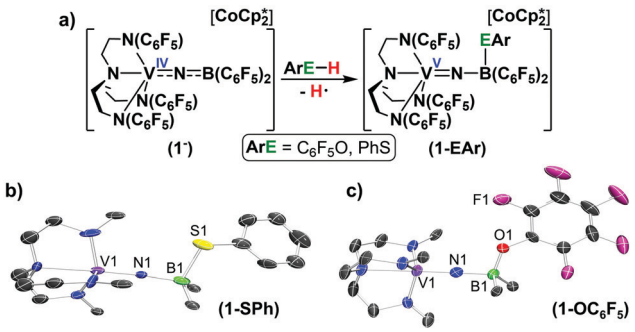

Fig. 2 (a) Reaction of $\mathbf{1}^-$ with C_6F_5OH or PhSH yielding **1-OC$_6$F$_5$** or **1-SPh**, respectively. (b and c) Solid-state structures of the anions of (b) **1-SPh** and (c) **1-OC$_6$F$_5$** (tren-based C_6F_5 groups (except *ipso* carbons), hydrogen atoms, $[CoCp^*_2]^+$ counter-cations, and co-crystallized solvent molecules are omitted for clarity). Selected bond lengths (Å) and angles (°): V1–N1 (1.661(avg) (**1-SPh**); 1.655(7) (**1-OC$_6$F$_5$**)), N1–B1 (1.535(avg) (**1-SPh**); 1.564(11) (**1-OC$_6$F$_5$**)), B1–S1 (1.960(17)) (avg) (**1-SPh**), B1–O1 (1.476(10) (**1-OC$_6$F$_5$**)), V1–N1–B1 (172.7(avg) (**1-SPh**); 171.3(5) (**1-OC$_6$F$_5$**)).

suggesting that while N–H CIBW may be less pronounced in this case, spontaneous H• ejection may still occur and lead to diamagnetic V-based products. The ^{1}H NMR spectrum also revealed tren-based resonances and shifted *o*-, *m*-, and *p*-PhNH peaks. Addition of a HAA agent in the form of half an equivalent of Gomberg's dimer ($Ph_2C(C_6H_5)CPh_3 \rightleftharpoons 2\ Ph_3C^\bullet$) or TEMPO radical resulted in a significantly cleaner reaction along with concomitant production of the Ph_3C–H or TEMPO–H products as observed by ^{1}H NMR spectroscopy (Fig. S50–S52, ESI†). The broad resonance centered at −312 ppm in the ^{51}V NMR spectrum, as well a set of 6 resonances in the ^{19}F NMR spectrum both pointed to the formation of the product, **1-NHPh**, analogous to those above (Fig. 2). This was unambigiously confirmed by XRD studies which further revealed a B(1)–N(2)HPh bond length (1.515(6) Å) consistent with an amide (Fig. S70, ESI†).[27] These results point to significant N–H CIBW of over 20 kcal mol^{-1} (Table 1) and suggest a separated CPET mechanism is likely at play (Fig. 1).

We next targeted NH_3 where metal-mediated N–H CIBW to various metal centers has been shown to enable spontaneous H_2 evolution[5] or catalytic HAA chemistry to produce N_2.[4] Exposure of **1**$^-$ to stoichiometric NH_3 (0.4 M THF solution) in bromobenzene resulted in a complex mixture of products, likely a result of the high N–H BDFE rendering its activation more difficult (Fig. S53, ESI†). Nonetheless, we successfully identified a major product, **1-NH**, by single-crystal XRD studies (Fig. 3a and d). We attribute the formation of **1-NH** to initial formal loss of H• from the proposed intermediate, **[1-NH$_3$]***, followed by intramolecular S_NAr cyclization of the following intermediate, **[1-NH$_2$]***, to generate **1-NH** (Fig. 3a). The solid-state structure of **1-NH** again revealed a significantly shortened V1═N1 bond (1.635(3) Å) indicative of oxidation to V^V.[17] The product also featured a broad resonance in the ^{51}V NMR spectrum at −274 ppm, similar to **1-SPh** (−272 ppm) and **1-OC$_6$F$_5$** (−302 ppm). The ^{19}F NMR spectrum revealed a complicated set of at least 9 resonances (some broadened) attributed to the general lack of molecular symmetry and the presence of rotationally restricted C_6F_5 rings due to observed π–π stacking in the solid-state structure (Fig. S71, ESI†).

The reaction sequence from **1**$^-$ to **1-NH** proposed in Fig. 3a suggests that CIBW of ammonia's N–H bonds resulted in spontaneous H• ejection. However, we note that under these conditions: (1) the fate of the released H• remains unclear, and; (2) several other products are formed, some of them unknown. We sought additional clarity on the mechanism of this reaction to address some of these points. First, we observed that addition of an HAA agent (TEMPO, $Ph_3C^\bullet$) – producing the observed TEMPO–H or Ph_3C–H products (Fig. S54, ESI†) – resulted in a significantly faster reaction, similar to previous observations.[5] We propose that a separated CPET mechanism may be facilitated under these conditions (Fig. 1). With TEMPO, this would indicate that CIBW leads to a drop of >30 kcal mol^{-1} in the N–H BDFE of ammonia upon coordination to B (*i.e.* **[1-NH$_3$]***, Fig. 3a and Table 1). Second, some of the other identifiable by-products formed in this reaction included C_6F_5H (similar to the $PhNH_2$ case (*vide supra*)), as well as **2**. The generation of the

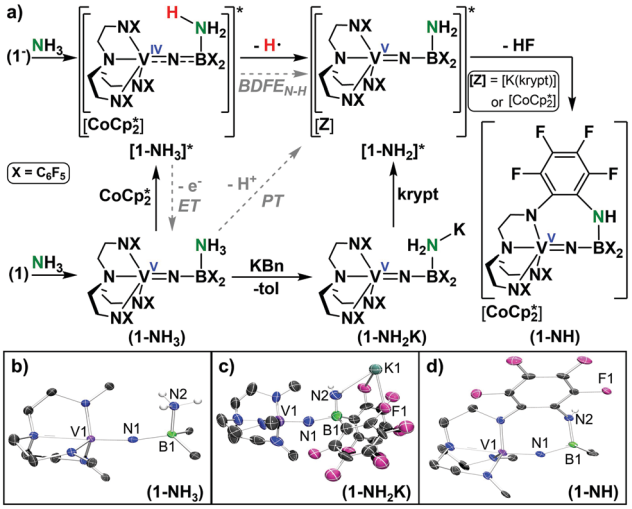

Fig. 3 (a) Reactivity of **1**$^-$ with NH_3 generating **1-NH** as the major product *via* the proposed intermediates, **[1-NH$_3$]'** and **[1-NH$_2$]'**. The reactions of **1-NH$_3$** with $CoCp^*_2$ or **1-NH$_2$K** with Kryptofix-222 (krypt) similarly yield **1-NH** as the major product. Solid-state structures of: (b) **1-NH$_3$**; (c) **1-NH$_2$K**, and; (d) the anion of **1-NH** (tren-based C_6F_5 groups (except *ipso* carbons and except one in **1-NH**), hydrogen atoms (except N–H), $[CoCp^*_2]^+$ counter-cation (for **1-NH**), and co-crystallized solvent molecules are omitted for clarity). Selected bond lengths (Å) and angles (°): V1–N1 (1.6557(19) (**1-NH$_3$**); 1.652(8) (**1-NH$_2$K**); 1.635(3) (**1-NH**)), N1–B1 (1.535(3) (**1-NH$_3$**); 1.607(14) (**1-NH$_2$K**); 1.528(6) (**1-NH**)), B1–N2 (1.611(3) (**1-NH$_3$**); 1.503(14) (**1-NH$_2$K**); 1.554(6) (**1-NH**)), V1–N1–B1 (168.24(16) (**1-NH$_3$**); 164.4(7) (**1-NH$_2$K**); (155.6(3) (**1-NH**)).

minor V^V by-product, **2**, from the reaction of **1**$^-$ with **NH$_3$** may suggest competing unknown disproportionation side reactions and/or reactions with the *in situ*-generated HF (Fig. 3a).

To support the intermediacy of **[1-NH$_3$]*** in the generation of **1-NH**, we first synthesized the V^V ammonia congener, **1-NH$_3$**, from **1** (Fig. 3a). This species was fully characterized, including by XRD studies (Fig. 3b). We next exposed **1-NH$_3$** to $CoCp^*_2$ and observed the clean formation of the product, **1-NH**, as well as some C_6F_5H (Fig. S56–S59, ESI†). We suspect the latter may form due to unknown side reactions involving the released H•. Next, to support the intermediacy of **[1-NH$_2$]*** in the generation of **1-NH**, we synthesized a potassium salt variant of **1-NH$_3$**, termed **1-NH$_2$K**, through deprotonation of the former using benzyl potassium (KBn, Fig. 3a). The solid-state structure of **1-NH$_2$K** (Fig. 3c) revealed a contracted B1–N2 bond (1.503(14) Å) relative to the B1–N2 bond in **1-NH$_3$** (1.611(3) Å; Fig. 3b) consistent with amide *vs.* amine coordination, respectively. Furthermore, in addition to the single H_2N–K bond, the K^+ cation was primarily supported by a network of at least 8 F–K contacts (only 2 shown in Fig. 3c) from two neighboring **1-NH$_2$K** molecules, as seen in the extended structure. Removing the K^+ cation from this coordination sphere by addition of the cryptand, 4,7,13,16,21,24-hexaoxa-1,10-diazabicyclo[8.8.8] hexacosane (Kryptofix-222 = krypt), resulted in the rapid intramolecular S_NAr cyclization reaction to generate **1-NH** – presumably *via* the intermediate **[1-NH$_2$]*** – as observed by multinuclear (^{51}V, ^{19}F, ^{11}B, ^{1}H) NMR spectroscopy (Fig. 3a and Fig. S60–S63, ESI†). Compound **2** was also produced in this reaction and is likely due

to protonation of the starting material or intermediate by the *in situ* generated HF.

The Bordwell equation (eqn (1)) is commonly used to experimentally determine E–H BDFEs of substrate undergoing PCET reactions (stepwise or concerted).[1,28]

$$\mathrm{BDFE_{sol}(E{-}H)} = 1.37\mathrm{p}K_a + 23.06E^\circ + C_{\mathrm{G,sol}} \quad (1)$$

In order to estimate the N–H BDFE in the proposed intermediate, **[1-NH$_3$]***, we applied this equation using the partial square scheme marked by the dashed gray arrows in Fig. 3a and using **1-NH$_3$** as our starting compound. In this case, the pK_a of **1-NH$_3$** is needed for the PT step, and the reduction potential (E°) of the $V^{V/IV}$ couple, **1-NH$_3$**/**[1-NH$_3$]***, for the ET step. To determine these values, these experiments were performed in MeCN due to the abundance of known pK_as in this solvent (C_G is a solvent-specific constant = 54.9 kcal mol^{-1} in MeCN). First, the pK_a of **1-NH$_3$** was experimentally bracketed using the known bases, piperidine and 1,8-diazabicyclo[5.4.0]undec-7-ene (DBU) (Fig. S64 and S65, ESI†). While no reaction was observed with the former, a reaction was observed with the latter yielding the product **1-NH** – through the proposed **[1-NH$_2$]*** intermediate – as observed by NMR spectroscopy. These data provide a bracketed pK_a value for **1-NH$_3$** between 19.35 < pK_a < 24.31. Second, the reduction potential (E°) for the **1-NH$_3$**/**[1-NH$_3$]*** couple was determined using cyclic voltammetry (CV). For organic solutions, reversible $E_{1/2}$ values *vs.* the ferrocene/ferrocenium (Fc/Fc$^+$) couple are typically used as a measure of E°.[1] The CV of **1-NH$_3$** (1.5 mM) was collected in MeCN with [Bu$_4$N][PF$_6$] (0.1 M) as supporting electrolyte and revealed an irreversible reduction event at $E^{\mathrm{red}}_{\mathrm{peak}} = -1.87$ V *vs.* Fc/Fc$^+$ at a scan rate of 250 mV s^{-1} (Fig. S75, ESI†). Increasing the scan rate up to 5 V s^{-1} did not yield a return oxidative feature. These data are of little surprise given the proposed intermediacy of the reduced product, **[1-NH$_3$]***, and likely point to an EC-type mechanism on the electrochemical timescale. While a reversible $E_{1/2}$ value could not be extracted, even at fast scan rates, it is nonetheless appropriate to use the $E^{\mathrm{red}}_{\mathrm{peak}}$ value as an approximate value of E° in eqn (1).[1,28,29] Thus, combining these experimental data (pK_a, E°, C_G), we conservatively estimate a bracketed N–H BDFE in **[1-NH$_3$]*** to be 38.3 kcal mol^{-1} < BDFE$_{\mathrm{N-H}}$ < 45.1 kcal mol^{-1}. These data are consistent with the observed facile separated CPET reactivity observed with HAA agents, such as TEMPO and Ph$_3$C$^\bullet$ (Table 1), as well as the spontaneous ejection of H$^\bullet$ in the absence of these reagents.

In summary, we have described the substantial CIBW (>30 kcal mol^{-1}) of a series of E–H bonds upon coordination to the vanadium-tethered boron complex, **1**$^-$, leading to facile PCET chemistry. Utilizing such main group/metal platforms may allow for the decoupling and tuning of the pK_a and $E_{1/2}$ parameters through judicious choice of main group Lewis acid and neighboring metal redox center, thereby allowing for a systematic approach to lowering substrate E–H BDFEs.

We thank the National Science Foundation (CHE-1900651) and the U.S.-Israel Binational Science Foundation (2018221) for funding.

Conflicts of interest

There are no conflicts to declare.

Notes and references

1 J. J. Warren, T. A. Tronic and J. M. Mayer, *Chem. Rev.*, 2010, **110**, 6961–7001.
2 J. W. Darcy, B. Koronkiewicz, G. A. Parada and J. M. Mayer, *Acc. Chem. Res.*, 2018, **51**, 2391–2399.
3 I. Pappas and P. J. Chirik, *J. Am. Chem. Soc.*, 2016, **138**, 13379–13389.
4 P. L. Dunn, S. I. Johnson, W. Kaminsky and R. M. Bullock, *J. Am. Chem. Soc.*, 2020, **142**, 3361–3365.
5 M. J. Bezdek, S. Guo and P. J. Chirik, *Science*, 2016, **354**, 730–733.
6 M. Paradas, A. G. Campaña, T. Jiménez, R. Robles, J. E. Oltra, E. Buñuel, J. Justicia, D. J. Cárdenas and J. M. Cuerva, *J. Am. Chem. Soc.*, 2010, **132**, 12748–12756.
7 H. Fang, Z. Ling, K. Lang, P. J. Brothers, B. de Bruin and X. Fu, *Chem. Sci.*, 2014, **5**, 916–921.
8 M. J. Bezdek and P. J. Chirik, *Angew. Chem., Int. Ed.*, 2018, **57**, 2224–2228.
9 D. P. Estes, D. C. Grills and J. R. Norton, *J. Am. Chem. Soc.*, 2014, **136**, 17362–17365.
10 K. T. Tarantino, D. C. Miller, T. A. Callon and R. R. Knowles, *J. Am. Chem. Soc.*, 2015, **137**, 6440–6443.
11 E. C. Gentry and R. R. Knowles, *Acc. Chem. Res.*, 2016, **49**, 1546–1556.
12 Z. Wang, S. I. Johnson, G. Wu and G. Ménard, *Inorg. Chem.*, 2021, **60**, 8242–8251.
13 J. Rittle and J. C. Peters, *J. Am. Chem. Soc.*, 2017, **139**, 3161–3170.
14 P. Bhattacharya, Z. M. Heiden, G. M. Chambers, S. I. Johnson, R. M. Bullock and M. T. Mock, *Angew. Chem., Int. Ed.*, 2019, **58**, 11618–11624.
15 M. D. Zott, P. Garrido-Barros and J. C. Peters, *ACS Catal.*, 2019, **9**, 10101–10108.
16 F. G. Bordwell, *Acc. Chem. Res.*, 1988, **21**, 456–463.
17 A. Wong, J. Chu, G. Wu, J. Telser, R. Dobrovetsky and G. Ménard, *Inorg. Chem.*, 2020, **59**, 10343–10352.
18 M. Keener, M. Peterson, R. Hernández Sánchez, V. F. Ostwald, G. Wu and G. Ménard, *Chem. – Eur. J.*, 2017, **23**, 11479–11484.
19 U. Mayer, V. Gutmann and W. Gerger, *Monatsh. Chem.*, 1975, **106**, 1235–1257.
20 M. A. Beckett, G. C. Strickland, J. R. Holland and K. Sukumar Varma, *Polymer*, 1996, **37**, 4629–4631.
21 I. B. Sivaev and V. I. Bregadze, *Coord. Chem. Rev.*, 2014, **270–271**, 75–88.
22 E. A. Mader, V. W. Manner, T. F. Markle, A. Wu, J. A. Franz and J. M. Mayer, *J. Am. Chem. Soc.*, 2009, **131**, 4335–4345.
23 G. J. P. Britovsek, J. Ugolotti and A. J. P. White, *Organometallics*, 2005, **24**, 1685–1691.
24 P. A. Chase, A. L. Gille, T. M. Gilbert and D. W. Stephan, *Dalton Trans.*, 2009, 7179–7188.
25 M. A. Dureen, G. C. Welch, T. M. Gilbert and D. W. Stephan, *Inorg. Chem.*, 2009, **48**, 9910–9917.
26 C. Schneider, J. H. W. LaFortune, R. L. Melen and D. W. Stephan, *Dalton Trans.*, 2018, **47**, 12742–12749.
27 A.-M. Fuller, A. J. Mountford, M. L. Scott, S. J. Coles, P. N. Horton, D. L. Hughes, M. B. Hursthouse and S. J. Lancaster, *Inorg. Chem.*, 2009, **48**, 11474–11482.
28 F. G. Bordwell, J. P. Cheng and J. A. Harrelson, *J. Am. Chem. Soc.*, 1988, **110**, 1229–1231.
29 F. G. Bordwell, J. Cheng, G. Z. Ji, A. V. Satish and X. Zhang, *J. Am. Chem. Soc.*, 1991, **113**, 9790–9795.

